Unlock your experimental potential
with power and agility
BD FACSymphony™ A5 SE Cell Analyzer
Discover the difference >

BD

The Journal of Immunology

This information is current as of February 24, 2022.

Large TCR Diversity of Virus-Specific CD8 T Cells Provides the Mechanistic Basis for Massive TCR Renewal after Antigen Exposure

Isabelle Miconnet, Angélique Marrau, Alex Farina, Patrick Taffé, Selena Vigano, Alexandre Harari and Giuseppe Pantaleo

J Immunol 2011; 186:7039-7049; Prepublished online 9 May 2011;
doi: 10.4049/jimmunol.1003309
http://www.jimmunol.org/content/186/12/7039

Supplementary Material http://www.jimmunol.org/content/suppl/2011/05/09/jimmunol.1003309.DC1

References This article **cites 53 articles**, 28 of which you can access for free at:
http://www.jimmunol.org/content/186/12/7039.full#ref-list-1

Why *The JI*? Submit online.

- **Rapid Reviews! 30 days*** from submission to initial decision
- **No Triage!** Every submission reviewed by practicing scientists
- **Fast Publication!** 4 weeks from acceptance to publication

**average*

Subscription Information about subscribing to *The Journal of Immunology* is online at:
http://jimmunol.org/subscription

Permissions Submit copyright permission requests at:
http://www.aai.org/About/Publications/JI/copyright.html

Email Alerts Receive free email-alerts when new articles cite this article. Sign up at:
http://jimmunol.org/alerts

The Journal of Immunology is published twice each month by
The American Association of Immunologists, Inc.,
1451 Rockville Pike, Suite 650, Rockville, MD 20852
Copyright © 2011 by The American Association of Immunologists, Inc. All rights reserved.
Print ISSN: 0022-1767 Online ISSN: 1550-6606.

Downloaded from http://www.jimmunol.org/ by guest on February 24, 2022

Large TCR Diversity of Virus-Specific CD8 T Cells Provides the Mechanistic Basis for Massive TCR Renewal after Antigen Exposure

Isabelle Miconnet,* Angélique Marrau,* Alex Farina,* Patrick Taffé,[†,‡] Selena Vigano,* Alexandre Harari,*[,§] and Giuseppe Pantaleo*[,§]

Ex vivo analysis of virus-specific CD8 T cell populations by anchored PCR has shown that the CD8 TCR repertoire was less oligoclonal (seven to nine clonotypes per individual epitope) than previously thought. In the current study, TCR diversity was investigated by assessing both the overall TCR β-chain variable regions usage as well as the CDR3 regions in ex vivo-isolated CMV- and EBV-specific CD8 T cells from 27 healthy donors. The average number of clonotypes specific to most single viral epitopes comprised between 14 and 77. Changes in the CD8 TCR repertoire were also longitudinally assessed under conditions of HIV-1 chronic infection (i.e., in patients with suppressed virus replication and after treatment interruption and Ag re-exposure). The results showed that a large renewal (≤80%) of the TRB repertoire occurred after Ag re-exposure and was eventually associated with an increased T cell recognition functional avidity. These results demonstrate that the global CD8 TCR repertoire is much more diverse (≤9-fold) than previously estimated and provide the mechanistic basis for supporting massive repertoire renewal during chronic virus infection and Ag re-exposure. ***The Journal of Immunology*****, 2011, 186: 7039–7049.**

T cells, particularly CD8 T cells, play a crucial role in antiviral immunity, and both quantitative and qualitative features of the CD8 T cell response are critical for virus control and protection. Whereas the features of virus-specific CD8 T cell responses have been extensively explored at phenotypic and functional levels, limited information is available on the structural characterization of the TCR repertoire emerging after virus infection in vivo. In this regard, the adaptive T cell response has evolved to generate a large number of T cells able to recognize diverse antigenic epitopes through TCRs (1). The TCR repertoire is potentially extremely diverse as a consequence of the combinatorial rearrangement of TCR genes and the imprecise recombination during these rearrangements. CDR3 encoded by the imprecise rearrangement of V, D, and J gene segments is involved in TCR contact with peptide–MHC (pMHC) complex.

Despite its potential diversity, several studies have shown that the TCR repertoire emerging in response to antigenic stimulation is restricted. Independently of the Ag selection process during the course of an immune response, mechanisms involved during thymic selection contribute to limit the TCR repertoire diversity (2, 3). Although the mechanisms have not been clearly established (reviewed in Refs. 4, 5), the limited pattern of epitopes recognized among the large number of potent immunogenic epitopes encoded by viruses (immunodominant epitopes) is an important factor for the limitation of the TCR repertoire diversity (6–9). Furthermore, in several situations, certain virus epitopes recruited a low number of clonotypes (reviewed in Ref. 10). This phenomenon was extensively demonstrated for the EBV- and flu-derived epitopes selecting public sequences (6, 11), respectively. Crystallographic studies revealed structural constraints of TCR–pMHC interaction as responsible for the highly restricted TCR repertoire in response to these two epitopes (12, 13). It has also been proposed that successive and repetitive stimulation upon chronic infection might be responsible for TCR repertoire narrowing (14, 15). However, the idea of repertoire narrowing is not consensual either in experimental models or during HIV infection (16–18). In addition, it has been shown that the TCR repertoire directed against a particular CMV-derived epitope remained quite heterogeneous in healthy individuals (15). Along the same line, direct sequencing of the TCR β-chain by anchored PCR on ex vivo virus-specific sorted CD8 T cells revealed that two epitopes derived from EBV and CMV were recognized by CD8 T cells exhibiting a higher degree (seven to nine clonotypes) of clonotypic diversity (19, 20) indicating that the TCR repertoire during viral response might not be as restricted as thought. The variable degree of diversity of the TCR repertoire observed during chronic virus infections might be related to the experimental strategies used in various studies. Many studies have analyzed the TCR repertoire in T cell lines and/or clones obtained in vitro from a limited number of subjects (21, 22) and/or have been based on the use of an incomplete panel of anti-Vβ mAbs (14, 15, 21–23), raising the question of to what extent these data were representative of the

*Division of Immunology and Allergy, Department of Medicine, University Hospital Center, University of Lausanne, 1011 Lausanne, Switzerland; [†]Health Care Evaluation Unit, Institute for Social and Preventive Medicine, University of Lausanne, 1011 Lausanne, Switzerland; [‡]Swiss HIV Cohort Study, University of Lausanne, 1011 Lausanne, Switzerland; and [§]Swiss Vaccine Research Institute, 1011 Lausanne, Switzerland

Received for publication October 6, 2010. Accepted for publication April 11, 2011.

This work was partially supported by research grants from the Swiss National Science Foundation (FN-310030-116342 and FN-310030-130692). This research was partially conducted as part of the Vaccine Immune Monitoring Consortium under the Collaboration for AIDS Vaccine Discovery with support from the Bill & Melinda Gates Foundation.

Address correspondence and reprint requests to Dr. Isabelle Miconnet or Prof. Giuseppe Pantaleo, Division of Immunology and Allergy, University Hospital Center, University of Lausanne, Beaumont 29, 1011 Lausanne, Switzerland. E-mail addresses: Isabelle.miconnet@chuv.ch and Giuseppe.pantaleo@chuv.ch

The online version of this article contains supplemental material.

Abbreviations used in this article: IMGT, ImMunoGeneTics; MNCs, mononuclear cells; PI, prediction interval; pMHC, peptide–MHC; pMHCI, peptide–MHC class I; TI, treatment interruption; TRB, TCR-β chain repertoire; TRBC, TCR-β–chain C region; TRBV, TCR-β–chain V region.

Copyright © 2011 by The American Association of Immunologists, Inc. 0022-1767/11/$16.00

www.jimmunol.org/cgi/doi/10.4049/jimmunol.1003309

Downloaded from http://www.jimmunol.org/ by guest on February 24, 2022

in vivo situation. With regard to the direct sequencing of the TCR β-chain by anchored PCR in ex vivo Ag-specific sorted cells (19, 20, 24), it is possible that the TCR repertoire diversity might be underestimated, as the degree of diversity measured will be dependent upon the extent of sequencing with the potential for preferential detection of dominant CD8 T cell clonotypes.

The primary objective of the current study was to evaluate the degree of TCR diversity of CD8 T cells specific to viruses establishing chronic infections. We have investigated CMV and EBV infections because these two viruses infect a large proportion (60–98%) of individuals and the virus-specific memory CD8 T cell responses can be readily detected ex vivo. Furthermore, we also monitored the changes of the TCR repertoire occurring over time in HIV-1–infected subjects experiencing large increments in viremia levels between, before, and after antiviral therapy interruption. To avoid the risk of culture bias, the TCR repertoire of virus-specific CD8 T cells was analyzed ex vivo in sorted virus-specific CD8 T cells using fluorescent peptide–MHC class I (pMHCI) pentamers. Because CDR3 regions are involved in the TCR interaction with pMHC complex, we focused on TCR β-chain and CDR3β variation (hereafter referred to as TRB repertoire) as a measure of the diversity of an Ag-driven TCR repertoire. To circumvent the caveats of selecting for the most represented clonotypes within Ag-specific T cell populations, CDR3β diversity was evaluated in the sorted pMHCI pentamers$^+$ virus-specific CD8 T cells within all the TCR-β–chain V regions families identified by PCR. Our results indicate that the global TRB repertoire of virus-specific CD8 T cells is greatly diverse and undergoes massive renewal after Ag re-exposure.

Materials and Methods

Patients

HIV-1–infected patients no. 1023, no. 1016, and no. 1042 were diagnosed with primary infection and treated with AZT plus 3TC plus LPV/RTV upon enrollment in the HIV-1 Primary Infection cohort Lausanne study (25). The patients underwent treatment interruption, and an HIV-1 viral rebound was subsequently monitored. Samples of 100 ml blood were collected at several time points after obtaining written informed consent of the patients. The study was approved by the Institutional Review Board of the Centre Hospitalier Universitaire Vaudois.

Isolation of cells and selection of samples

Blood samples were obtained from the local blood bank (Lausanne, Switzerland). Blood mononuclear cells (MNCs) were isolated from whole blood samples from healthy donors by Ficoll-Hypaque density gradient centrifugation. Samples were screened for the presence of epitope-specific CD8 T cells by flow cytometry using pMHCI pentamers (Proimmune, Oxford, U.K.) and CD3- and CD8-specific mAbs (BD Biosciences, Erembodegem, Belgium). The fluorescence was measured using an LSRII flow cytometer (BD Biosciences). Samples from HIV-1–infected patients were mapped for the presence of CD8 T cells with a panel of 194 optimal HIV-derived epitopes (26) organized in a matrix setting. Epitope mapping was confirmed by flow cytometry when pMHCI pentamer was available. Patient no. 1023 responded to four epitopes (HLA-B*0702/p24$_{223–231–GPGHKARVL}$, HLA*0301/p17$_{20–28–RLRPGGKK}$, HLA*B0702/gp160$_{843–851–IPRRIRQGL}$, and HLA*B13/nef$_{106–114–RQDILDLWI}$), patient no. 1016 to three epitopes (HLA-A*0201/RT$_{309–317–ILKEPVHGV}$, HLA-A*0201/p17$_{77–85–SLYNTVATL}$, and HLA*A0201/gp120$_{90–98–KLTPLCVTL}$), and patient no. 1042 to three epitopes (HLA-B*4001/p6$_{33–41–KELYPLTSL}$, HLA-B*0801/p24$_{128–135–EIYKRWII}$, and HLA*B4001/RT$_{5–12–IETVPVKL}$).

Detection of IFN-γ intracellular production

Blood MNCs from HIV-1–infected patients were stimulated overnight with 1 μg/ml of the cognate peptide in the presence of 1 μg/ml GolgiPlug (BD Biosciences). Cells were washed, permeabilized, and stained with CD8–PerCP–Cy5.5, CD4–FITC, and IFN-γ–allophycocyanin (BD Pharmingen, San Diego, CA). Data were acquired on an LSRII flow cytometer. The magnitude of specific T cell response was evaluated by measuring the percentage of IFN-γ–producing CD8 T cells. A response was considered positive when the percentage of cytokine-producing cells in stimulated samples was at least 5-fold greater than that in unstimulated samples.

Functional avidity of T cell recognition

Blood MNCs from HIV-1–infected patients were stimulated overnight by serial dilutions of the cognate peptide ranging from 1 μg/ml to 1 pg/ml in the presence of 1 μg/ml GolgiPlug (BD Biosciences). The specific T cell response was evaluated by measuring the percentage of IFN-γ–producing CD8 T cells by flow cytometry as above or using the IFN-γ ELISPOT assay as previously described (27). The functional avidity of the T cell responses was assessed by determining the peptide concentration capable of inducing half-maximal responses (EC_{50}).

Frequency of TRBV populations within Ag-specific T cells

Blood MNCs were stained with cognate pMHCI pentamers for 20 min at 4°C, washed, and then incubated with a mixture of CD8, CD3 mAbs (BD Biosciences) and Vβ mAbs (IOTest β Mark; Beckman Coulter, Marseille, France) for 20 min at 4°C. Data were acquired on an LSRII flow cytometer.

Cell sorting and RNA extraction

Blood MNCs were stained with cognate pMHCI pentamers for 20 min at 4°C, washed, and then incubated with a mixture of anti-CD8, anti-CD45RA, and anti-CCR7 mAbs (BD Biosciences). CD45RA$^+$ CCR7$^+$ naive and pMHCI pentamers$^+$ CD8$^+$ T cells were directly sorted (FACSAria; BD Biosciences) in RLT lysis buffer (Qiagen, Hilden, Germany) containing 20 ng RNA carrier (Roche Diagnostics, Rotkreuz, Switzerland) and RNA extracted (Qiagen).

cDNA amplification, TCR spectratyping and sequencing

cDNA preparation and amplification were performed by using the Super SMART PCR cDNA Synthesis Kit according to the manufacturer's instructions (Clontech Laboratories, Saint-Germain-en-Laye, France). Amplified cDNA was subjected to TRBV–TCR-β–chain C region (TRBC) PCR reactions using a set of twenty-four 5′ sense primers specific for the twenty-two TRBV families (28) and one 3′ antisense FAM-labeled primer specific for TRBC (5′-AGATCTCTGCTTATGGCTC-3′). For spectratyping, aliquots of positive samples were mixed with Genescan-500 ROX size standards and run on an ABI 3130 capillary sequencer (Applied Biosystems, Foster City, CA). To analyze further the CDR3 junction, TRBV product was purified, ligated into pGEM-T Easy Vector (Promega, Madison, WI), cloned by transformation of competent DH5a *Escherichia coli*, and sequenced with an M13 forward primer. The TRBV nomenclature is according to Wei et al. (29) and the international ImMunoGeneTics (IMGT) information system (http://www.imgt.org) (indicated in brackets in Figs. 2, 3, and 6). The CDR3 junction, length and sequence, was analyzed using the IMGT system.

Statistical analysis

To estimate the number of clonotypes emerging in response to the different CMV- and EBV-derived epitopes, the following analysis was performed. The data have a hierarchical structure with the individuals nested in epitopes (i.e., a two-level structure). Therefore, the hierarchical log-normal Poisson and log-normal negative binomial I and II mixture count regression models were investigated, and the best-fitting model was assessed (30, 31). Three predictive factors for the clonotype count were considered: at level one, the number of TRBV sequenced and the number of CDR3 fragments found were treated as fixed factors, whereas at level two, the epitope category was treated as random. We used both a frequentist and a Bayesian approach to assess proper convergence of the MCMC Bayesian algorithm (32, 33). In the Bayesian formulation, noninformative zero mean normal priors were postulated for the level one regression coefficients, and a noninformative zero mean normal prior was used for the level two random coefficient with a noninformative uniform distribution with support 1–100 hyper-prior for the SD between epitopes. The best functional for the two fixed factors was assessed using the fractional polynomial methodology (34). The regression model was first calibrated using the data set containing the partial number of clonotypes determined based on the partial sequencing of TRBV. Then, 95% confidence (for the mean number) and prediction intervals for the predictive number of clonotypes, given complete sequencing of TRBV as well as CDR3 level and epitope, were calculated. The prediction intervals were calculated using the 2.5 and 97.5% quantiles of the posterior predictive distribution for the Bayesian model. The hierarchical log-normal Poisson regression model turned out to be the most appropriate as the overdispersion coefficient was found to be almost null ($\alpha = 0.02$). The best functional form for TRBV was found to be

Downloaded from http://www.jimmunol.org/ by guest on February 24, 2022

of the form $\beta_1 \times 1/TRBV^2 \times \log(TRBV) + \beta_2 \times 1/TRBV^2$, whereas it was linear for CDR3. Prediction intervals based on Chebyshev's inequality are well known to be conservative and too large. All the calculations were performed using WinBUGS version 1.4.3 and STATA version 11.1.

Results

CDR3 length distribution analysis of TRBV transcripts derived from CMV- and EBV-specific CD8 T cells isolated from healthy subjects

According to the approach outlined in Supplemental Fig. 1, the detailed analysis of TRBV usage and CDR3 length profile for each TRBV subfamily emerging in response to CMV-derived epitopes was performed in healthy donors responding to HLA-B*0702/CMV-pp65$_{417–426–TPRVTGGGAM}$ and HLA-A*0201/CMV-pp65$_{495–503–NLVPMVATV}$ (hereafter referred to as CMV$_{TPRVTGGGAM}$ and CMV$_{NLVPMVATV}$, respectively). The representative profiles obtained in three of five donors are shown in Fig. 1*A*. In control naive CD8 T cells, PCR amplification was obtained for each pair of TRBV–TRBC primers, and the CDR3 length patterns displayed an average of eight peaks distributed in a Gaussian-like fashion (data not shown). Although more restricted than the one observed in naive cells, the TRBV repertoire of CMV-specific CD8 T cells was diverse and heterogeneous between individuals (Fig. 1*A*). Thirteen to 21 and 15 to 22 TRBV subfamilies were detected in CMV$_{NLVPMVATV}$- and CMV$_{TPRVTGGGAM}$-specific CD8 T cells, respectively, without preferential usage. Most TRBV families were composed of a lower number of CDR3 length peaks compared with naive cells (Fig. 1*A* and data not shown). Cumulative data presented in Fig. 1*C* indicated that 7–21 (median 14) and 7–22 (median 15) TRBV subfamilies were detected in CMV$_{NLVPMVATV}$- and CMV$_{TPRVTGGGAM}$-specific CD8 T cells, respectively. Moreover, 14–54 (median 29) and 11–55 (median 22) CDR3 fragments were observed in these specific CD8 T cells, respectively.

Consistently with the pattern observed for CMV-specific CD8 T cells, similar TRBV usage and CDR3 length patterns were also observed in CD8 T cells specific to two of three EBV-derived epitopes. The TRBV repertoires of HLA-B*0801/EBV-BZFL1$_{190–197–RAKFKQLL}$ (EBV$_{RAKFKQLL}$) and HLA-B*0801/EBV-BMLF1$_{259–267–GLCTLVAML}$ (EBV$_{GLCTLVAML}$) specific CD8 T cells were diverse and heterogeneous between individuals (Fig. 1*B*). Cumulative data indicated that 9–21 (median 13) TRBV were detected in response to EBV$_{RAKFKQLL}$ and 8–22 TRBV (median 15) were observed in CD8 T cells specific to EBV$_{GLCTLVAML}$ (Fig. 1*C*). Similar to CMV-specific CD8 T cells, TRBV families detected in response to these two EBV-derived epitopes were mostly composed of a low number of CDR3 size peaks (Fig. 1*B* and data not shown). As for CMV-specific CD8 T cells, a higher number of total CDR3 fragments was found in response to both EBV$_{RAKFKQLL}$ (15–59, median = 21) and EBV$_{GLCTLVAML}$ (11–58, median = 24) (Fig. 1*C*).

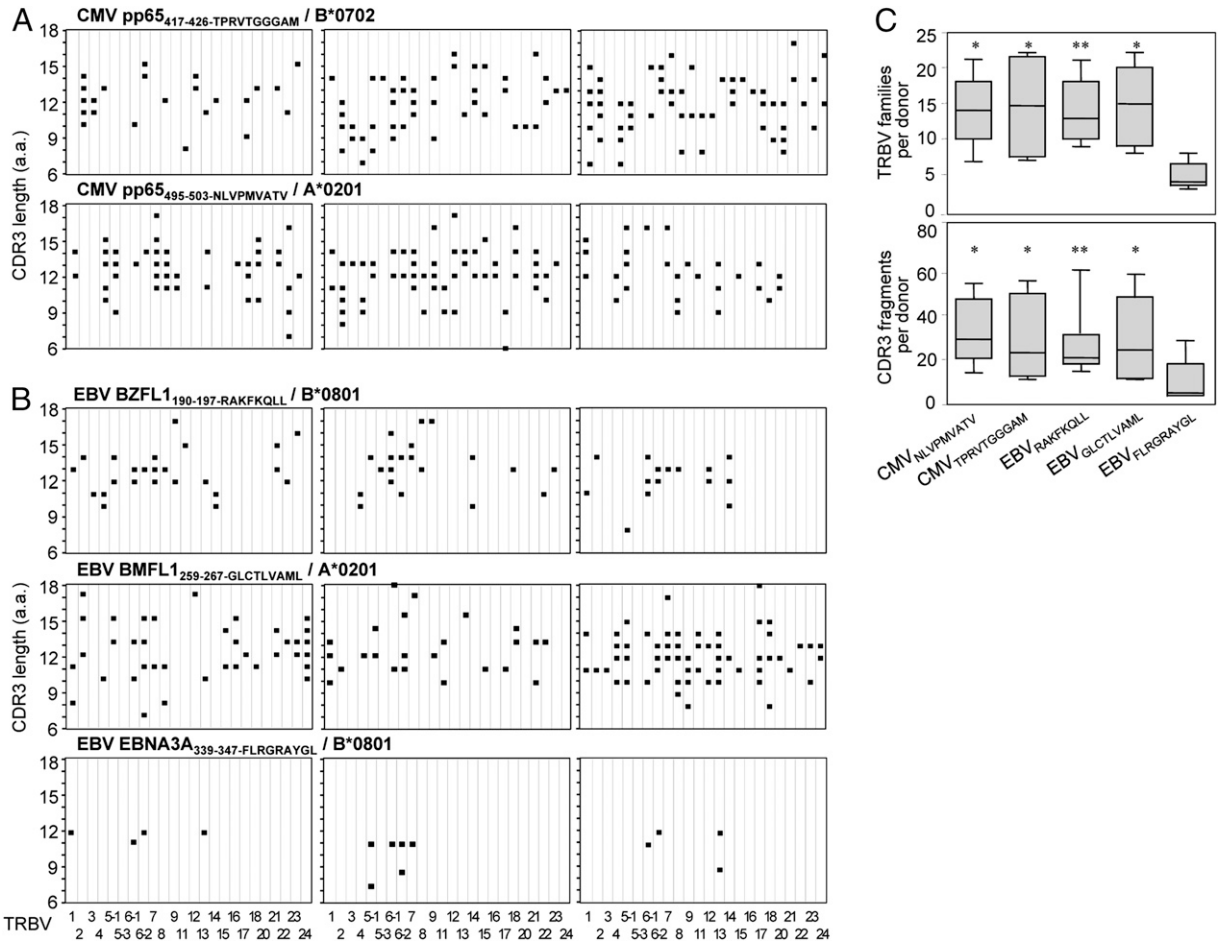

FIGURE 1. CDR3 length distribution analysis of TRBV transcripts derived from CMV- and EBV-specific CD8 T cells isolated from healthy subjects. *A* and *B*, The CDR3 length distribution of TRBV transcripts was determined in (*A*) CMV- and (*B*) EBV-specific CD8$^+$ T cells. The CDR3 fragments found in the different TRBV subfamilies are represented by squares and their lengths indicated in amino acids. *C*, The cumulative data of the median number of TRBV families and CDR3 length fragments generated from 27 healthy donors with CD8 T cells specific to CMV- and EBV-derived epitopes are shown. $*p < 0.05$, $**p < 0.005$ (Kruskal–Wallis test).

Downloaded from http://www.jimmunol.org/ by guest on February 24, 2022

Different from what was found with these two EBV-derived epitopes, the CD8 T cells specific to HLA-B*0801/EBV-EBNA3A$_{339–347–FLRGRAYGL}$ (EBV$_{FLRGRAYGL}$) were far more restricted (Fig. 1*B*). Overall, 3–8 TRBV (median 4) and 4–28 (median 5) CDR3 fragments were detected in response to this epitope in five healthy subjects (Fig. 1*C*). Of note, only one CDR3 size peak of 11 aa was detected in the TRBV6.1 subfamily in four of five subjects.

Clonotypic diversity in response to CMV- and EBV-derived epitopes in healthy subjects

We next assessed the clonotypic diversity of CD8 T cells specific to CMV- and EBV-derived epitopes. The large TRBV and CDR3 length diversity shown above led us to focus on several selected TRBV subfamilies. In particular, we further analyzed some TRBV families presenting CDR3 length peaks shared by different subjects. The clonotypic diversity was also assessed within a few TRBV families with a CDR3 length peaks profile more restricted to individual subjects. TRBV PCR products were cloned, and 10 clones were sequenced per each CDR3 size. This number of clones allowed us in most cases to obtain by sequencing the same CDR3 sizes as those defined by spectratyping. In particular, the most and the less represented CDR3 length fragments were confirmed by sequencing (in 100% and >80% of TRBV, respectively), indicating that the sample number (10 clones) analyzed was representative of the TRBV population and thus suitable for determining the clonotypic diversity (Supplemental Fig. 1*C*). Overall, a median number of 79 sequences (range 43–208) was obtained per donor responding to CMV$_{TPRVTGGGAM}$, CMV$_{NLVPMVATV}$, EBV$_{RAKFKQLL}$, and EBV$_{GLCTLVAML}$. Ten to 92 sequences (median 20) were obtained per donor responding to EBV$_{FLRGRAYGL}$. The sequence analysis of the TRBV subfamilies selected revealed substantial clonotypic diversity (Figs. 2, 3). Even though most TRBV families detected in response to CMV-specific epitopes presented dominant clonotypes, most TRBV families and also CDR3 length fragments were composed of more than one CDR3 junctional region (Fig. 2). In addition, no consensus CDR3 motifs were identified, but one GSSG motif at CDR3 position 5 was observed in the TRBV14 subfamily in two subjects responding to CMV$_{TPRVTGGGAM}$. The conservation of this N-encoded sequence suggested Ag-driven selection of this clonotype. Of note, two clonotypes found in response to CMV$_{NLVPMVATV}$ were also found by anchored RT-PCR and sequencing of subclones in previous studies (19, 20). With regard to EBV-specific CD8 T cells, the same degree of clonotypic diversity was found for two epitopes (Fig. 3). Notably, some CDR3 motifs and even sequences were conserved between individuals responding to EBV$_{RAKFKQLL}$ (Fig. 3). A partly N-encoded motif GE at CDR3 position 5 was observed in the TRBV4 subfamily from five of six subjects. Moreover, a particular CDR3 sequence TRBV14-TRBJ1-1 CASSSLNTEAFF was detected in four of five individuals indicating the existence of a public repertoire in response to EBV$_{RAKFKQLL}$. This public clonotype dominated the CD8 T cell response in three of four of these individuals. The fact that these conserved CDR3 motifs and public CDR3 sequences were encoded by distinct nucleotide sequences within one individual and/or by non-germline sequences suggests Ag-driven

CMV pp65$_{417-426-TPRVTGGGAM}$ / HLA-B*0702

TRBV	ID	Junction	TRBD	TRBJ	CDR3 length	Frequency
6.2 (7-9)	AM19	CASSLRQGANTGELFF	1*01	2-2*01	14	14/30
		CASSLRQGANAGELFF	1*01	2-2*01	14	1/30
		CASSLRQGINTGELFF	1*01	2-2*01	14	4/30
		CASSSHDLAGVKSEQFF	2*02	2-1*01	15	10/30
		CASSPPLGSGSGDEKLFF	1*01	1-4*01	16	1/30
	AM17	CASSAGTGIYDEAFF	1*01	1-1*01	13	20/32
		CASSAGTGIYDGAFF	1*01	1-1*01	13	1/32
		CASSLIGVSSYNEQFF	2*01	2-1*01	14	11/32
	CD40-29	CASSLRGENRDDYEQYF	2*01	2-7*01	15	11/19
		CASSLRGESLVNEQFF	2*01	2-1*01	14	5/19
		CASSLKGVGQSDEQYF	2*02	2-7*01	14	1/19
		CASSLISGRARNEQFF	2*02	2-1*01	14	1/19
		CASSFRGEGHPDTQYF	2*02	2-3*01	14	1/19
	KEL-12	CASSSHEDRGSSSPLHF	1*01	1-6*02	15	13/17
		CASSSHDKQGARSPLHF	1*01	1-6*02	15	2/17
		CASSARQGIDTGELFF	1*01	2-2*01	14	1/17
		CASSLIGQGLGDEQFF	1*01	2-1*01	14	1/17
	AM41	CASSLLQGARTEAFF	1*01	1-1*01	13	16/34
		CASSLLQGARTEAFF	1*01	1-1*01	13	3/34
		CASSSRDRGAYEQYF	1*01	2-7*01	13	6/34
		CASSRRGESSYNEQFF	2*01	2-1*01	14	3/34
		CASSLRGVSSYNEQFF	2*01	2-1*01	14	6/34
13 (6-1) (6-5)	AM17	CASSDQSQETQYF	?	2-5*01	11	8/8
	CD40-29	CASSYSTVNEQFF	2*01	2-1*01	11	10/10
14 (27)	AM19	CASRVGGAGNSPLHF	1*01	1-6*01	13	2/33
		CASSLSWGGFYNEQFF	2*01	2-1*01	14	28/33
		CASSLAWGGFYNEQFF	2*01	2-1*01	14	1/33
		CASSLSWGGFYNEQLF	2*01	2-1*01	14	1/33
		CAGSLSWGGFYNEQFF	2*01	2-1*01	14	1/33
	AM17	CASRQGAGGNQPQHF	1*01	1-5*01	13	19/38
		CASRLGPGQPYEQYF	1*01	2-7*01	13	12/38
		CASSLGSSGTRQYF	2*02	2-3*01	12	3/38
		CASSLLGLQGSYNEQFF	2*01	2-1*01	15	2/38
		CASRLGPGQPYERYF	1*01	2-7*01	13	1/38
		CASRSGPGQPYEQYF	1*01	2-7*01	13	1/38
	CD40-29	CASSLGSSGNEQFF	2*01	2-1*01	12	17/28
		CASSLGAGNYGYTF	1*01	1-2*01	12	10/28
		CATSIGSSGNEQFF	2*01	2-1*01	12	1/28
	KEL-12	CASSLSTSSRNYGYTF	1*01	1-2*01	14	10/19
		CASRTGAANIYEQYF	1*01	2-7*01	13	7/19
		CASRTGAANIYEQHF	1*01	2-7*01	13	2/19
	AM41	CASSLSPSTGNYGYTF	1*01	1-2*01	14	9/27
		CASSLGPGNYEQYF	2*01	2-7*01	12	5/27
		CASNTGGANTDTQYF	1*01	2-3*01	13	5/27
		CASSLGGSPNYGYTF	1*01	1-2*01	13	5/27
		CASRLGAAGSQPQHF	1*01	1-5*01	13	2/27
		CASPLIEETIPYEQYF	2*02	2-7*01	14	1/27

CMV pp65$_{495-503-NLVPMVATV}$ / HLA-A*0201

TRBV	ID	Junction	TRBD	TRBJ	CDR3 length	Frequency
1 (9)	AM22	CASSVAGSATGELFF	2*01	2-2*01	13	10/23
		CASSVGSEAYTYEQYF	2*02	2-7*01	14	12/23
		CASSPGTGREQFF	2*01	2-1*01	11	1/23
	AM35	CASSVGAGVFTDTQYF	2*02	2-3*01	14	12/18
		CASSGVGGTDTQYF	2*02	2-3*01	12	6/18
5.1 (5.1)	AM22	CASFRGHEQFF	1*01	2-1*01	9	11/34
		CASSLGLAATYNEQFF	2*01	2-1*01	14	6/34
		CASSWAGGPRDEQYF	2*01	2-7*01	13	5/34
		CASSTSLLAGNNEQFF	2*01	2-1*01	14	3/34
		CASSLMGPGQPQHF	1*01	1-5*01	12	2/34
		CASSLRQGEGMGEQFF	1*01	2-1*01	14	2/34
		CASSLSLLAGNNEQFF	2*01	2-1*01	14	1/34
		CASSWAGEPRDEQYF	2*01	2-7*01	13	1/34
		CARSWAGGPRDEQYF	1*01	2-7*01	13	1/34
		CASSCAGGPRDEQYF	2*01	2-7*01	13	1/34
		CASSLAGRETEAFF	1*01	1-1*01	12	1/34
	CD40-38	CASMNDGATYEQYF	2*01	2-7*01	12	21/27
		CASVNDGATYEQYF	2*01	2-7*01	12	1/27
		CASRSGTYDNSPLHF	1*01	1-6*?	13	5/27
	AM35	CASRALRGDNEQFF	2*01	2-1*01	12	20/22
		CASSDPDRAVTEAFF	1*01	1-1*01	13	2/22
6.2 (7-9)	AM22	CASSLDRDRGRPEAFF	1*01	1-1*01	14	32/32
	CD40-38	CASSLAERSYEQYF	2*01	2-7*01	12	25/27
		CASSLAPGATNEKLFF	1*01	1-4*01	14	2/27
	AM35	CASSFGQAWETQYF	1*01	2-5*01	12	21/26
		CASSFGQAWYEQYF	1*01	2-7*01	12	3/26
		CASSFGQAWYEQYF	1*01	2-7*01	12	1/26
		CASSLVGTGGWDEQFF	1*01	2-1*01	14	1/26
8 (12-3) (12-4)	AM22	CASSLSDRGGDEQFF	2*01	2-1*01	13	15/32
		CASRLGLGYEQYF	2*01	2-7*01	11	8/32
		CASSFYSSGRNSYF	2*02	2-3*01	12	5/32
		CASSLRPLDMNTEAFF	1*01	1-1*01	14	2/32
		CASSLAPGDGYEQYF	2*01	2-7*01	13	1/32
		CASGLSDRGGDEQFF	2*01	2-1*01	13	1/32
	CD40-38	CASSSVNEQFF	1*01	2-1*01	9	8/15
		CASSPGSSFYGYPF	1*01	1-2*01	12	7/15
	AM35	CASSLTSEQFF	1*01	2-1*01	9	8/19
		CASSPGTLKETQYF	2*01	2-5*01	12	6/19
		CASSVVNEQFF	2*01	2-1*01	9	3/19
		CASSLTSEQFF	2*01	2-1*01	9	1/19
		CASSLTNEQFF	?	2-1*01	9	1/19
13 (6.1) (6.5)	AM22	CASSPLTGTGHYGYTF	1*01	1-2*01	14	6/10
		CASREGEYYGYTF	1*01	1-2*01	11	4/10
	CD40-38	CASSYQTGASYGYTF	1*01	1-2*01	13	9/9
	AM35	CASSYSTGIGGGYTF	1*01	1-2*01	13	17/26
		CASTPQTGTGTYGYTF	1*01	1-2*01	14	9/26

FIGURE 2. CDR3 sequences of CMV-specific CD8 T cells. CDR3 sequences were analyzed by using the IMGT system. Amino acid sequences derived from the germline nucleotidic sequences are underlined. Conserved CDR3 residues found in the current study are highlighted in yellow. Public clonotypes found in previous studies (19, 20) are shown in blue boxes.

Downloaded from http://www.jimmunol.org/ by guest on February 24, 2022

EBV BZFL1$_{190\text{-}197\text{-}RAKFKQLL}$ / HLA-B*0801

TRBV	ID	Junction	TRBD	TRBJ	CDR3 length	Frequency
4 (29-1)	AV	CSVGQGEDGPQHF	1*01	1-5*01	11	9/28
		CSTGSGEGYEQYF	1*01	1-5*01	11	11/28
		CSVGSGEDNEQFF	1*01	1-5*01	11	2/28
		CSVTSERTGTTWGYTF	1*01	1-5*01	14	1/28
		CSVTSERTGTNWGYTF	1*01	1-5*01	14	2/28
	AM7	CSAGTGEGGEQFF	1*01	2-1*01	11	17/22
		CSVGAGDYEQYF	2*01	2-1*01	10	2/22
		CSSGTGDGGEQFF	1*01	2-1*01	11	2/22
		CSAGTGEGGEQFF	2*01	2-1*01	11	1/22
	MCL-05	CSVGFGEGYEQYF	2*02	2-7*01	11	8/14
		CSVGQGGNYGYTF	1*01	1-2*01	11	3/14
		CSVKGGFPYNEQFF	2*01	2-1*01	12	3/14
	AM30	CSTGQGPYEQYF	1*01	2-7*01	10	31/33
		CSVGGVSSGVYNEQFF	2*01	2-1*01	14	2/33
	KEL-13	CSVGGGTEAFF	1*01	1-1*01	9	3/44
		CSGGQGEGEQFF	1*01	2-1*01	10	10/44
		CSGGQGEGEQFF	1*01	2-1*01	10	1/44
		CSGGQGEGEQYF	1*01	2-7*01	10	5/44
		CSGGQGGGGEQFF	1*01	2-1*01	10	1/44
		CSVGTGDNSPLHF	1*01	1-6*01	11	4/44
		CSVGSGEDNEQFF	2*01	2-1*01	11	5/44
		CSYSPGQGRNEQFF	1*01	2-1*01	12	2/44
		CSAGQGEGEQYF	1*01	2-7*01	10	3/44
		CSVKGTNTEAFF	1*01	1-1*01	10	1/44
		CSVKGQGTEAFF	1*01	1-1*01	10	1/44
		CSVETGDEKLFF	1*01	1-4*01	10	1/44
		CSVTAGEDDTQYF	2*01	2-3*01	11	1/44
		CSVTAGEDQPQHF	1*01	1-5*01	11	1/44
		CSVGPGENGPQHF	1*01	1-2*01	12	5/44
	AM42	CSVGAGEGYEQYF	2*02	2-7*01	11	10/17
		CSVGAGEGGPQHF	1*01	1-5*01	11	7/17
14 (27)	AV	CASSSLNTEAFF *	2*?	1-1*01	10	18/19
		CASSLDGRQVNQPQHF	1*01	1-5*01	14	1/19
	AM7	CASSSLNTEAFF *	?	1-1*01	10	9/20
		CASSSLNTEAFF *	1*01	1-1*01	10	2/20
		CASSPSGANVLTF	?	2-6*01	11	8/20
		CASSSPNTEAFF	?	1-1*01	10	1/20
	MCL-05	CASSSLNTEAFF *	1*01	1-1*01	10	6/16
		CASSSLNTEAFF *	?	1-1*01	10	7/16
		CASSSLDTEAFF	?	1-1*01	10	1/16
		CASSLLGGGYAYEQYF	2*01	2-7*01	14	2/16
	AM23	CASSSLNTEAFF *	2*?	1-1*01	10	24/30
		CASSSLNTEAFF *	1*01	1-1*01	10	2/30
		CACSSLNTEAFF	1*01	1-1*01	10	1/30
		CAGSSLNTEAFF	1*01	1-1*01	10	1/30
		CASSTRGGWVEAFF	1*01	1-1*01	12	1/30
		CASSSLSTEAFF	?	1-1*01	10	1/30
	AM42	CASSLLTGHEQFF	1*01	2-1*01	11	17/29
		CASSPSGANVLTF	?	2-6*01	11	7/29
		CASSLIPGDYYGYTF	1*01	1-2*01	13	3/29
		CASSPLTDTQYF	?	2-3*01	10	2/29

EBV BMLF1$_{259\text{-}267\text{-}GLCTLVAML}$ / HLA-A*0201

TRBV	ID	Junction	TRBD	TRBJ	CDR3 length	Frequency
2 (20-1)	041208	CSARDGTGNGYTF	1*01	1-2*01	11	4/10
		CSARDGTGNGYTF	1*01	1-2*01	11	3/10
		CSARDGTGNGYTF	1*01	1-2*01	11	2/10
		CSARGGTGNGYTF	1*01	1-2*01	11	1/10
	AM28	CSARSGVGNTIYF	1*01	2-3*01	11	9/10
		CSARDRVGNTIYF	1*01	2-3*01	11	1/10
	KEL-5	CSARDRTGNTIYF	1*01	1-3*01	11	7/21
		CSARSEVGNTIYF	?	1-3*01	11	2/21
		CSARDRTGNGYTF	1*01	1-2*01	11	4/21
		CSARVEPGNGYTF	1*01	1-2*01	11	6/21
		CSARSEVGDTIYF	1*01	1-3*01	11	1/21
		CSARDSTGNGYTF	1*01	1-2*01	11	1/21
	KEL-13	CSAHRTENTEAFF	1*01	1-1*01	11	6/9
		CSARDGTGNGYTF	1*01	1-2*01	11	2/9
4 (29-1)	AV	CSVGGTFYGYTF *	1*01	1-2*01	10	9/10
		CSVGTGGTNEKLFF	1*01	1-4*01	10	1/10
	041208	CSVPGTDYNEQFF	1*01	2-1*01	11	17/17
	AM28	CSVDLANTEAFF	1*01	1-1*01	10	12/27
		CSVDLANTEAFF	1*01	1-1*01	10	2/27
		CSVDLANAEAFF	1*01	1-1*01	10	1/27
		CSVGTGGTNEKLFF	1*01	1-4*01	12	6/27
		CSVGQGGTNEKLFF	1*01	1-4*01	12	5/27
		CSVQEGGYGYTF	1*01	1-2*01	10	1/27
	KEL-5	CSVGSGGTNEKLFF	1*01	1-4*01	12	16/17
		CSVGSGGTNERLFF	1*01	1-4*01	12	1/17
	KEL-13	CSVGGTFYGYTF *	1*01	1-2*01	10	12/42
		CSVEASGGLFNEQFF	2*01	2-1*01	13	8/42
		CSATDSMNTEAFF	1*01	1-1*01	11	5/42
		CSVPGQVLETQYF	1*01	2-5*01	11	5/42
		CSVEYSPTLYNEQFF	2*01	2-1*01	13	4/42
		CSVPSLLNTEAFF	?	1-1*01	11	3/42
		CSVGTGGTNEKLFF	1*01	1-4*01	12	3/42
		CSAPSLLNTEAFF	?	1-1*01	11	1/42
		CSVEASEGLFNEQFF	2*01	2-1*01	13	1/42

EBV EBNA3A$_{339\text{-}347\text{-}FLRGRAYGL}$ / HLA-B*0801

TRBV	ID	Junction	TRBD	TRBJ	CDR3 length	Frequency
1 (9)	AV	CASSPSAAAYEQYF	2*01	2-7*01	12	12/12
	AM7	CASSPRTLGTEAFF	1*01	1-1*01	12	16/16
6.1 (7-8)	AM7	CASSLGQAYEQYF	1*01	2-7*01	11	19/21
		CASSLGQAYEQYF	1*01	2-7*01	11	2/21
	AM30	CASSLGQAYEQYF	1*01	2-7*01	11	13/22
		CASSLGQAYEQYF	1*01	2-7*01	11	2/22
		CASSLGQAYEQYF	1*01	2-7*01	11	7/22
	AM23	CASSLGQAYEQYF	1*01	2-7*01	11	4/7
		CASSTGQAYEQYF	1*01	2-7*01	11	3/7

FIGURE 3. CDR3 sequences of EBV-BZFL1, -BMLF1, and -EBNA3A–specific CD8 T cells. CDR3 sequences were analyzed by using the IMGT system. Amino acid derived from the germline nucleotidic sequences are underlined. Conserved CDR3 residues found in the current study are highlighted in yellow and clonotypes shared between different individuals indicated by an asterisk. Public clonotypes found in previous studies (19, 20) are shown in blue boxes.

clonal selection. With regard to the T cell repertoire specific to EBV$_{GLCTLVAML}$, one new public clonotype was found in two donors, AV and KEL-13 (Fig. 3). Several other clonotypes defined in the current study were previously reported (19, 20). Concerning the EBV$_{FLRGRAYGL}$-specific CD8 T cells, we focused on the TRBV1 subfamily shared by two individuals and, more interestingly, on the TRBV6.1 subfamily detected in four of five subjects (Fig. 3). The TRBV1 subfamily contained one CDR3 length fragment and was composed of one particular clonotype different in each individual. The TRBV6.1 subfamily was also composed of one CDR3 length fragment. This fragment was composed of one public clonotype, TRBV6.1-TRBJ2-7 CASSLGQAYEQYF, dominant and shared by the three subjects analyzed, and one codominant private clonotype in one of these three subjects. As mentioned above for CD8 T cells specific to EBV$_{RAKFKQLL}$, this public clonotype was encoded by distinct nucleotide sequences within one individual (different germline-encoded amino acids underlined) and/or by non-germline sequences suggesting an Ag-driven clonal selection (Fig. 3). Of note, this public clonotype was already reported as a dominant CDR3 sequence in response to this EBV epitope (6).

We also evaluated the diversity of the TRB repertoire of high (dominant) versus low (subdominant) represented TRBV CD8 T cell populations responding to CMV and EBV epitopes and also measured the frequency of the TRBV populations within pentamer$^+$ CD8 T cells (Fig. 4*A*). In most cases, the TRBV populations identified by PCR were not detected by the commercially available anti-Vβ mAbs (Fig. 4*B*). However, the TRBV repertoire of the totality or a fraction (≥10% of pentamer$^+$ CD8 T cells) of dominant versus subdominant populations of Ag-specific CD8 T cells was possible in four of seven subjects. In subject no. AM35, CMV$_{NLVPMVATV}$-specific CD8 T cells were composed of 15% TRBV11, 53% TRBV13, and 30% TRBV23. In response to CMV$_{TPRVTGGGAM}$, 12% of specific CD8 T cells expressed TRBV14 in subject no. AM19 and 10% in subject no. KEL12. In response to EBV$_{GLCTLVAML}$, the majority of pentamer$^+$ CD8 T cells expressed TRBV2 (76%) and 5% expressed TRBV1, TRBV13, and TRBV22. With regard to their TRB diversity, both dominant and subdominant TRBV populations showed similar diversity either in terms of the number of CDR3 fragments and/or clonotypes (Fig. 4*B*). For instance, in subject no. AM35, the dominant TRBV11, 13, and 23 specific to CMV$_{NLVPMVATV}$ had the same number of CDR3 fragments and clonotypes compared with the subdominant TRBV1 and 5.1 populations. These results indicate that there was no bias in the TRB repertoire diversity between dominant and subdominant TRBV populations.

Estimation of TRB repertoire diversity in response to CMV- and EBV-derived epitopes

On the basis of the large data set generated by the analysis of the TRB repertoire in CMV- and EBV-specific CD8 T cells, we then explored the possibility of developing a mathematical model to

Downloaded from http://www.jimmunol.org/ by guest on February 24, 2022

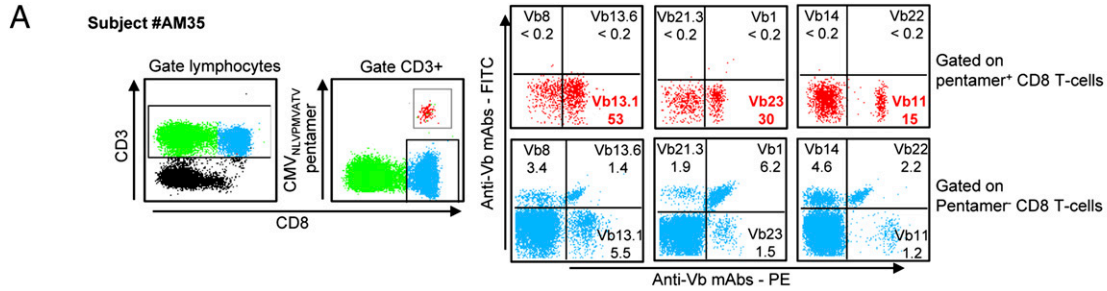

B

		TRBV 1	2	3	4	5.1	5.3	6.1	6.2	7	8	9	11	12	13	14	15	16	17	18	20	21	22	23	24
CMV pp65-NLVPMVATV / A*0201																									
AM35	Frequency	<0.2	<0.2	<0.2	<0.2	<0.2		-	-	<0.2	<0.2	<0.2	15	<0.2	53	<0.2	-	<0.2	<0.2	<0.2		<0.2	<0.2	30	
	CDR3	2	5	1	3	2		2	2	4	2	4	2	4	2	2	2	2	2	3		4	2	2	
	clonotypes	2				2			4		5		2		2									1	
AM22	Frequency	<0.2			<0.2	<0.2		-	-	<0.2	<0.2	<0.2			<0.2			1	<0.2	<0.2		<0.2	<0.2	<0.2	
	CDR3	3			5	4		1	1	6	4	2			2			1	3	4		2	4	1	
	clonotypes	3				11			1		6				2			1							
CMV pp65-TPRVTGGGAM / B*0702																									
AM19	Frequency			<0.2	<0.2				-		<0.2	<0.2			<0.2	12	-								
	CDR3			2	1				3		2	2			1	2	1								
	clonotypes			4	3				5		2	2			1	5	1								
KEL12	Frequency					<0.2			-			<0.2				10					<0.2			<0.2	
	CDR3					2			2			1				2					1			2	
	clonotypes								4			1				3								2	
EBV BZFL1-RAKFKQLL / B*0801																									
AM7	Frequency	<0.2	<0.2	<0.2	<0.2	<0.2		-	-	<0.2	<0.2	<0.2	1		<0.2	<0.2						1	<0.2	<0.2	
	CDR3	1	1	1	2	2		2	1	3	1	2	1		1	2						2	1	1	
	clonotypes		1		3			3	2	3	3		1			3						2			
AM30	Frequency		<0.2		<0.2	<0.2		-	-	<0.2	<0.2	<0.2			<0.2							<0.2	<0.2		
	CDR3		1		2	2		2	1	1	1	1			2							3	1		
	clonotypes		4		2	3		2	1	3	1	1			5							5	1		
EBV BMFL1-GLCTLVAML / A*0201																									
AM28	Frequency	1	76		<0.2						<0.2	<0.2			1							<0.2	3		
	CDR3	2	1		2						1	1			2							1	1		
	clonotypes	2	2		5										4								2		

FIGURE 4. Frequency of TRBV subsets within specific CD8 T cells and TRB diversity. *A*, Blood MNCs from subject no. AM35 were stained with allophycocyanin-labeled HLA-A*0201/$CMV_{NLVPMVATV}$ pentamer and a mixture of anti-CD3, anti-CD8, and anti-Vβ mAbs. $CD3^+$ T cells (in green) were selected within viable lymphocytes. The percentages of each TRBV population were determined within pMHCI $pentamer^+$ (in red) and pMHCI $pentamer^-$ (in blue) $CD8^+$ T cells as control. $CD3^-$ T cells are represented in black. *B*, The frequency of TRBV subpopulation within pMHCI $pentamer^+$ CD8 T cells is shown in the square. TRBV populations represented at a percentage ≥10% of pMHCI $pentamer^+$ CD8 T cells are shown in boxes. The number of CDR3 fragments is shown for each TRBV population detected by PCR. The number of clonotypes determined for the sequenced TRBV is also shown. TRBV for which anti-Vβ mAbs were not available are represented in red.

predict the TRB repertoire diversity of Ag-specific CD8 T cells. For this purpose, the data on the numbers of TRBV, CDR3 fragments, and clonotypes per each sequenced TRBV were analyzed using a hierarchical regression count model. Three predictive factors for the number of clonotypes were considered. The number of TRBV and CDR3 were treated as fixed factors, and the type of epitopes was treated as random (see *Materials and Methods*). The average number of clonotypes was thus predicted for an individual responding to a specific Ag and presenting a given number of TRBV and CDR3 fragments (Fig. 5). The level of diversity appeared highly heterogeneous between individuals and depended on the number of TRBV (Fig. 5 and data not shown). For instance, in response to $CMV_{NLVPMVATV}$, an average number of 14 clonotypes with a 95% prediction interval (PI) comprising between 6 and 23 was predicted in the subject presenting 7 TRBV, whereas an average number of 51 clonotypes was estimated in the subject presenting 21 TRBV (PI comprising between 30 and 76). Although variable, the level of TRB repertoire diversity remained elevated in response to the two CMV-derived epitopes and to $EBV_{RAKFKQLL}$ and $EBV_{GLCTLVAML}$ epitopes. In subjects responding to $CMV_{NLVPMVATV}$ and to $CMV_{TPRVTGGGAM}$, the average number of clonotypes ranged between 14 and 51 and between 16 and 62, respectively. The average value of clonotypes carried by CD8 T cells specific to $EBV_{RAKFKQLL}$ and $EBV_{GLCTLVAML}$ epitopes comprised between 24 and 77, and 17 and 64, respectively. In agreement with what was previously reported, the TRB repertoire specific to $EBV_{FLRGRAYGL}$ was far more restricted with only 4 to 22 estimated clonotypes per individual.

To validate this prediction strategy, we analyzed the clonotypic distribution within all TRBV families detected in response to one epitope in three randomly selected donors. The three donors responded to $CMV_{TPRVTGGGAM}$, $EBV_{RAKFKQLL}$, and $EBV_{FLRGRAYGL}$, and complete sequencing of the 8, 11, and 4 TRBV families specific to these epitopes was performed. As shown in Fig. 6, the number of clonotypes detected after complete sequencing in response to $CMV_{TPRVTGGGAM}$ and $EBV_{RAKFKQLL}$ was 23 and 27, respectively, whereas only 5 clonotypes were found in response to $EBV_{FLRGRAYGL}$. According to the prediction strategy, an average number of 17 (PI comprising between 7 and 26), 26 (PI comprising between 14 and 39), and 7 (PI comprising between 1 and 12) clonotypes were expected in response to $CMV_{TPRVTGGGAM}$, $EBV_{RAKFKQLL}$, and $EBV_{FLRGRAYGL}$, respectively. The actual clonotypes found by complete sequencing of the TRBV families specific to these three epitopes were thus

Downloaded from http://www.jimmunol.org/ by guest on February 24, 2022

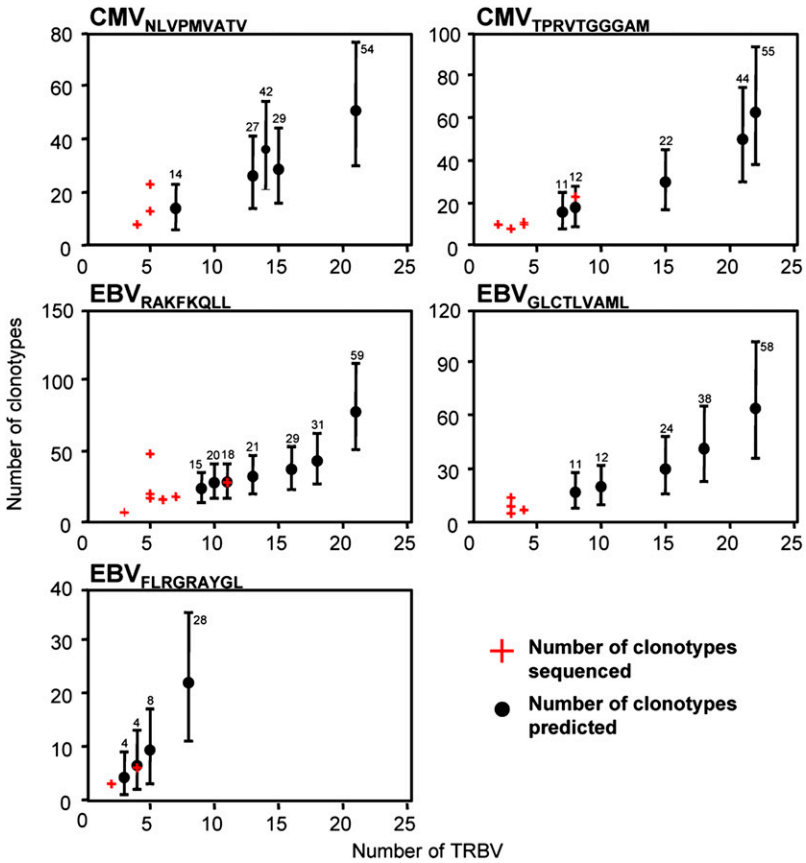

FIGURE 5. Estimation of clonotypic diversity within CMV- and EBV-specific CD8 T cells. The number of clonotypes determined from sequenced TRBV is indicated for each donor (red crosses). The average number of clonotypes predicted for the total TRBV defined is shown (black circles) for each individual as well as the 95% prediction interval. The number of CDR3 fragments for each individual is also indicated.

contained in the prediction intervals thereby confirming the reliability of the prediction model. Overall, these data provided validation and solid support for the use of this strategy for the estimation of the TRB diversity.

Changes in the TRB repertoire after Ag re-exposure

To evaluate further the TRB repertoire diversity in chronic virus infection and the changes occurring after Ag re-exposure, we performed a longitudinal analysis of TRBV and CDR3 diversity after treatment interruption (TI) and high levels of Ag re-exposure. Patients no. 1023, no. 1016, and no. 1042 were treated with antiviral therapy at the time of primary infection. All patients spontaneously decided to stop treatment ~2 y after the initiation of antiviral therapy and agreed to be monitored for viral load, CD4 T cell counts (Fig. 7*A*), and a series of immunological measures (Fig. 7*B*–*F*). TI was rapidly accompanied by HIV-1 viral load rebound and concomitant drop of CD4 T cell counts (Fig. 7*A*). TI was also associated with an increase of the number of CD8 T cell epitopes recognized in these patients (data not shown). The analysis of the TRB repertoire diversity was performed before and after TI. It has to be emphasized that the TRB repertoire was diverse in all patients (Fig. 7*B*, 7*C*). Before TI, 18, 19, and 21 TRBV and 39, 36, and 56 CDR3 fragments were detected in patient no. 1023, no. 1016, and no. 1042, respectively. Substantial changes in the TRB repertoire were observed in the three patients after TI and Ag re-exposure (Fig. 7*B*, 7*C*). The size of the TRB repertoire was slightly increased and/or stable in patients no. 1023 and no. 1042, respectively, whereas the TRB repertoire tended to narrow in patient no. 1016, this latter being characterized by the disappearance of 55% of TRBV and 72% of CDR3 fragments upon TI (Fig. 7*B*, 7*C*). The most striking changes were, however, observed in the quality of the repertoire, defined in this article as a measure of the renewal occurring between the two time points. Taking into account the concomitant disappearance of TRBV and CDR3 fragments from the first time point and the appearance of new TRBV and CD3 fragments at the second time point, the renewal of the TRB repertoire in patient no. 1023 was 18% for TRBV and 82% for CDR3 fragments, 60 and 88% in patient no. 1016, and 21 and 56% in patient no. 1042 (Fig. 7*B*, 7*C*).

The diversity and the renewal of the TRB repertoire before and after TI were further confirmed at the level of clonotypic composition. According to the prediction strategy validated above, an average number of 36 (PI comprising between 21 and 52), 42 (PI comprising between 28 and 58), and 52 (PI comprising between 32 and 76) clonotypes were expected in response to $p17_{SLYNTVATL}$, $p24_{GPGHKARVL}$, and $p6_{KELYPLTSL}$ in patients no. 1016, no. 1023, and no. 1042, respectively. The same level of diversity was estimated after TI with an average of 17 (PI 8–26), 57 (PI 39–78), and 44 (PI 26–65) clonotypes in response to $p17_{SLYNTVATL}$, $p24_{GPGHKARVL}$, and $p6_{KELYPLTSL}$ in patients no. 1016, no. 1023, and no. 1042. The renewal of the TRB repertoire was further confirmed by assessing the clonotypic diversity of CD8 T cells specific to $p24_{GPGHKARVL}$ and $p17_{SLYNTVATL}$ epitopes in patients no. 1023 and no. 1016. For these purposes, TRBV families presenting CDR3 length peaks shared between pre-TI and post-TI samples were sequenced. Consistently with the increased diversity of TRBV and CDR3 fragments over time (Fig. 7*B*, 7*C*), large changes in clonotypes were also observed in patient no. 1023 (Fig. 7*D*, Supplemental Fig. 2). The clonotypic composition of 6 of 12 TRBV analyzed (Fig. 7*D*, Supplemental Fig. 2) was completely changed after TI. Although one dominant clonotype was maintained over time in TRBV7, the six subdominant clonotypes were replaced by eight new clonotypes, representing 37 and 62% of the clonotypic repertoire, respectively. The profiles of dominant

Downloaded from http://www.jimmunol.org/ by guest on February 24, 2022

CMV pp65$_{417\text{-}426\text{-}TPRVTGGGAM}$ / HLA-B*0702

TRBV	Junction	TRBD	TRBJ	CDR3 length	Frequency
3 (28)	CASRRQRTDTEAFF	1*01	1-1*01	12	9/21
	CASRRQRTDAEAFF	1*01	1-1*01	12	1/21
	CASRHQRTDTEAFF	1*01	1-1*01	12	1/21
	CASSQRLAGAHEQYF	2*02	2-7*01	13	10/21
4 (29-1)	CSVIGGFGTGELFF	2*01	2-2*01	12	16/24
	CSVEERVRGGEQYF	2*01	2-7*01	12	3/24
	CSVEERVWGGEQYF	2*01	2-7*01	12	4/24
	CSVEERVWGGEQYF	2*01	2-7*01	12	1/24
6-2 (7-9)	CASSLRQGANTGELFF	1*01	2-2*01	14	14/30
	CASSLRQGANAGELFF	1*01	2-2*01	14	1/30
	CASSLRQGINTGELFF	1*01	2-2*01	14	4/30
	CASSSHDLAGVKSEQFF	2*02	2-1*01	15	10/30
	CASSPPLGSGSGDEKLFF	1*01	1-4*01	16	1/30
8 (12-3,12-4)	CASSYVIYEQYF	?	2-7*01	10	51/54
	CASSYVIYEQYF	?	2-7*01	10	1/54
	CASSHVIYEQYF	?	2-7*01	10	2/54
9 (3-1,3-2)	CASSQKGLDTEAFF	1*01	1-1*01	12	8/10
	CASGQKGLDTEAFF	1*01	1-1*01	12	2/10
13 (6-1,6-5)	CASSYSSGELFF	?	2-2*01	10	10/10
14 (27)	CASRVGGAGNSPLHF	1*01	1-6*01	13	2/33
	CASSLSWGGFYNEQFF	2*01	2-1*01	14	28/33
	CASSLAWGGFYNEQFF	2*01	2-1*01	14	1/33
	CASSLSWGGFYNEQLF	2*01	2-1*01	14	1/33
	CAGSLSWGGFYNEQFF	2*01	2-1*01	14	1/33
15 (24)	CATSDDRDTGELFF	1*01	2-2*01	12	16/16

EBV BZFL1$_{190\text{-}197\text{-}RAKFKQLL}$ / HLA-B*0801

TRBV	Junction	TRBD	TRBJ	CDR3 length	Frequency
2 (20-1)	CSARDRGAANTGELFF	1*01	2-2*01	14	6/16
	CSARDRGAENTGELFF	1*01	1-4*01	14	6/16
	CSAKDRGAENTGELFF	1*01	1-4*01	14	2/16
	CSARDREGGNSPLHF	1*01	1-6*01	13	1/16
	CSARDREGGNSPLHF	1*01	1-6*01	13	1/16
4 (29-1)	CSTGQGPYEQYF	1*01	2-7*01	10	31/33
	CSVGGVSSGVYNEQFF	1*01	2-1*01	14	2/33
5-1 (5-1)	CASSYSGGVFEQFF	2*01	2-1*01	12	9/19
	CASSLTAGNNYGYTF	1*01	1-2*01	13	9/19
	CASSLTAGNNCGYTF	1*01	1-2*01	13	1/19
6-1 (7-8)	CASSWLAGTREEQYF	2*01	2-7*01	13	17/18
	CASSGSGLVNTGELFF	2*01	2-2*01	14	1/18
6-2 (7-9)	CASSSTRTGDGQPQHF	1*01	1-5*01	14	9/9
7 (4-1)	CASSFGQGEGYEQYF	1*01	2-7*01	13	8/10
	CASSPGTGEGYEQYF	2*01	2-7*01	13	1/10
	CASSQEGQLSYEQYF	1*01	2-7*01	13	1/10
8 (12-3,12-4)	CASSPLAGVGETQYF	2*01	2-5*01	13	17/17
9 (3-1,3-2)	CASSLIRGTGELFF	1*01	2-2*01	12	9/9
13 (6-1,6-5)	CASSYPRGGEGSPLHF	1*01	1-6*02	14	12/20
	CASSYPWGGEGSPLHF	1*01	1-6*02	14	1/20
	CASNYPRGGEGSPLHF	1*01	1-6*02	14	1/20
	CASSPGGRQGDYNEQFF	2*01	2-1*01	15	6/20
21 (11-2)	CASSLLAGQETQYF	2*01	2-5*01	12	7/34
	CASSLSAGQETQYF	2*01	2-5*01	12	3/34
	CASSELAGVGETQYF	2*01	2-5*01	13	16/34
	CASSELAGVGETQYF	2*01	2-5*01	13	1/34
	CASSEPAGVGETQYF	2*01	2-5*01	13	1/34
	CASSSSSGASYNEQFF	1*01	2-1*01	14	6/34
22 (2)	CASSEQSGANVLTF	1*01	2-6*01	12	12/12

EBV EBNA3A$_{339\text{-}347\text{-}FLRGRAYGL}$ / HLA-B*0801

TRBV	Junction	TRBD	TRBJ	CDR3 length	Frequency
5-1 (5-1)	CASNQETQYF	?	2-5*01	8	30/31
	CASNQGTQYF	2*02	2-5*01	8	1/31
6-1 (7-8)	CASSLGQAYEQYF	1*01	2-7*01	11	13/22
	CASSLGQAYEQYF	1*01	2-7*01	11	2/22
	CASSLGQAYEQYF	1*01	2-7*01	11	7/22
6-2 (7-9)	CASSWGPEAFF	1*01	1-1*01	9	17/17
7 (4-1)	CASSQAGFNEQFF	2*01	2-1*01	11	16/16

FIGURE 6. Complete sequencing of CDR3 junction in three healthy individuals with CD8 T cells specific to CMV- and EBV-derived epitopes. HLA-B*0702/CMV-pp65$_{417–426–TPRVTGGGAM}$, HLA-B*0801/EBV-BZFL1$_{190–197–RAKFKQLL}$, and HLA-B*0801/EBV-EBNA3A$_{339–347–FLRGRAYGL}$ pentamer$^+$ CD8$^+$ T cells were sorted from three healthy individuals. CDR3 sequences were analyzed by using the IMGT system. Amino acids derived from the germline nucleotidic sequences are underlined. Public clonotypes are shown in blue boxes.

and subdominant clonotypes changed in TRBV1 and TRBV24 (Fig. 7*D*, Supplemental Fig. 2). The clonotype profiles remained stable only in 3 of 12 TRBV sequenced (Fig. 7*D*, Supplemental Fig. 2). In patient no. 1016, the narrowing of the TRB repertoire after TI was confirmed at the level of the clonotypic distribution. In TRBV5-1, there was disappearance of three subdominant clonotypes, whereas six clonotypes were replaced by two new clonotypes in TRBV13 (Fig. 7*D*, Supplemental Fig. 3). In TRBV17, one dominant and one subdominant clonotype became codominant, and two subdominant clonotypes were replaced by a new one (Fig. 7*D*, Supplemental Fig. 3). No changes were observed in TRBV24 (Fig. 7*D*, Supplemental Fig. 3).

Changes in the functional avidity of virus-specific CD8 T cells after TI

To investigate whether the large renewal in the TRB repertoire was associated with functional changes in the CD8 T cell responses directed against viral Ags, we investigated the functional avidity of the CD8 T cells specific to p24$_{GPGHKARVL}$, p17$_{SLYNTVATL}$, and p6$_{KELYPLTSL}$ in patients no. 1023, no. 1016, and no. 1042, respectively (Fig. 7*E*, 7*F*). In two of three patients, the magnitude of HIV-1–specific CD8 T cell response, as measured by the percentage of IFN-γ–producing CD8 T cells, strongly increased after TI (i.e., 17-fold in patient no. 1016 and 3.6-fold in patient no. 1042) (Fig. 7*E*). No changes were observed in patient no. 1023 (Fig. 7*E*). Functional avidity of the virus-specific CD8 T cells was measured on gated IFN-γ–producing CD8 T cells and analyzed on the samples before and after TI. In patient no. 1016, EC_{50} shifted from 7×10^{-4} μg/ml to 2×10^{-5} μg/ml and in patient no. 1042 from 1.5×10^{-3} μg/ml to 2.7×10^{-4} μg/ml after TI (Fig. 7*F*). No changes were observed in patient no. 1023 (Fig. 7*D*). Therefore, massive renewal in the CD8 T cells repertoire after Ag reexposure may be associated with substantial increase in the magnitude and in the functional avidity of the responding CD8 T cells.

Discussion

The majority of studies investigating the T cell repertoire elicited upon antigenic-specific stimulation has been based on the characterization of T cell lines and/or clones established in vitro, on a limited number of subjects, and by direct sequencing of the TCR β-chain by anchored PCR on ex vivo virus-specific sorted CD8 T cells. In this study, we have applied a multisteps strategy including 1) sorting of virus-specific pMHCI pentamer$^+$ CD8 T cell populations, 2) PCR analysis of TRBV usage within the sorted virus-specific CD8 T cells, 3) analysis of the CDR3 junction length by spectratyping, and 4) sequence analysis of CDR3 junctions in the TRBV families contained within the virus-specific CD8 T cells. We found that the global TRB repertoire emerging in response to most viral Ags studied was greatly diverse and the extent of the diversity much greater than that estimated in previous studies (19, 20). Of note, the concept of global CD8 TRB repertoire diversity reported in the current study coincides with the high CD8 TRB repertoire global diversity estimated in experimental models (35–38) and the broad range of CD8 T cell clonotypes reported in hepatitis-C–infected patients (39).

Downloaded from http://www.jimmunol.org/ by guest on February 24, 2022

A

	1023			1016			1042		
	Baseline	Pre-TI	Post-TI	Baseline	Pre-TI	Post-TI	Baseline	Pre-TI	Post-TI
Time points (week)	0	0 - 114	115 - 295	0	0 - 146	166 - 392	0	0 - 76	82- 136
Log10 HIV RNA copies/mL Median (range)	5.7	1.7 (1.7-3.6)	4.8 (4.0 – 5.3)	4.6	1.7 (1.7-3.9)	3.8 (1.7-4.8)	7.3	1.9 (1.3-5.7)	5.5 (1.3-5.9)
CD4 counts/μL Median (range)	447	941 (719-1181)	476 (306-776)	331	756 (566-1078)	570 (333-920)	295	870 (566-1078)	565 (211-910)

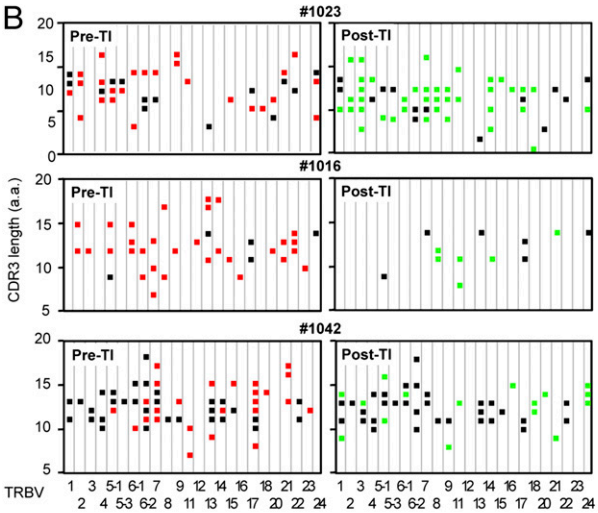

C

Patient	1023		1016		1042	
Time point	Pre-TI	Post-TI	Pre-TI	Post-TI	Pre-TI	Post-TI
TRBV	18	22	19	9	21	22
CDR3	39	53	36	12	56	47
TRBV shared	18		8		19	
TRBV new	4		1		3	
CDR3 shared	14		5		31	
CDR3 new	39		7		16	

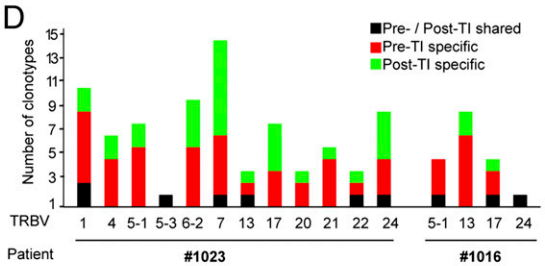

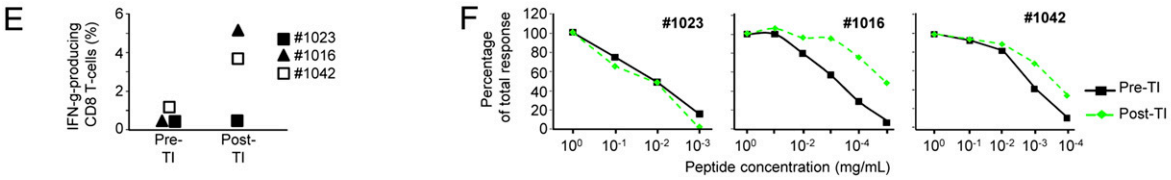

FIGURE 7. Longitudinal analysis of TRB repertoire in HIV-1–infected subjects. *A*, HIV-1 viremia levels and CD4 T cell counts in patients no. 1023, no. 1016, and no. 1042 at the time of diagnosis of primary infection and before and after TI. *B*, The CDR3 length distribution of TRBV transcripts in CD8$^+$ T cells specific to HLA-B*0702/p24$_{223–231–GPGHKARVL}$ (patient no. 1023), HLA-A*0201/p17$_{77–85–SLYNTVATL}$ (patient no. 1016), and HLA-B*4001/p6$_{33–41–KELYPLTSL}$ (patient no. 1042) HIV-1–derived peptides was analyzed before and after TI. CDR3 fragments found in different TRBV subfamilies are represented by squares and their length indicated in amino acids. Black squares correspond with CDR3 fragments shared by pre- and post-TI samples, and red and green squares correspond with CDR3 fragments found only in pre-TI and post-TI samples, respectively. *C*, The total number of TRBV and CDR3 fragments is shown for each time point. The numbers of TRBV and CDR3 fragments shared by pre- and post-TI samples or emerging de novo in post-TI samples are also indicated. *D*, The analyses of clonotypes found before and after TI in patients no. 1023 and no. 1016 were performed only on the TRBV shared by the two time points. The number of clonotypes shared by pre- and post-TI samples (black boxes) and specific for pre-TI (red boxes) and post-TI (green boxes) samples are depicted in each TRBV family. *E* and *F*, The magnitude (*E*) and the functional avidity (*F*) of T cell responses specific for HIV-1 HLA-B*0702/p24$_{223–231–GPGHKARVL}$ (patient no. 1023), HLA-A*0201/p17$_{77–85–SLYNTVATL}$ (patient no. 1016), and HLA-B*4001/p6$_{33–41–KELYPLTSL}$ (patient no. 1042) before and after TI are represented.

An average of seven to nine different clonotypes was previously shown in CD8 T cells specific to CMV$_{NLVPMVATV}$ and to EBV$_{GLCTLVAML}$ using anchored RT-PCR (19, 20). The global TRB repertoire measured in response to these and other epitopes derived from CMV and EBV lytic proteins in the current study had much greater diversity. The greater diversity was consistently observed by the analysis of different measures of TCR diversity. In particular, the average number of clonotypes specific to CMV- and EBV-derived lytic epitopes ranged between 14 and 77 clonotypes per single epitope. Therefore, the degree of estimated TRB diversity is ≤9-fold greater than that reported in previous studies (19, 20).

Combining the analysis of the CDR3 fragments with extensive sequencing of individual TRBV families, we have developed a strategy to estimate the TRB diversity without necessarily performing complete sequencing. This strategy was validated through the complete sequencing of the TRB repertoires measured in response to CMV$_{TPRVTGGGAM}$ and EBV$_{RAKFKQLL}$. Of note, this statistical model also presents the advantage to be applied to the prediction of the TRB repertoire diversity in response to any type of viral epitope. Indeed, the type of epitope was treated as random and the variability of parameters was taken into account for various virus-derived epitopes including HIV epitopes (data not shown).

The greater degree of TRB diversity in the current study compared with that of previous studies (19, 20) may result from the different experimental strategy used to determine the TRB repertoire diversity. The key difference is likely to screen the whole clonotypic distribution in TRBV families detected within one Ag-specific CD8 T cell population rather than performing direct ex vivo sequencing that may select for dominant clonotypes. This was supported by the measurement of the frequency of TRBV populations within Ag-specific T cells and by the absence of bias in TRB diversity in dominant and subdominant CD8 T cell populations. The larger diversity of the TRB repertoire shown in our study is in agreement with and helps to explain the broad range of avidities and of T cell clones recruited in response to microbial infection (40).

A more restricted TRB repertoire was found in response to EBV$_{FLRGRAYGL}$ epitope derived from EBNA3A latent protein, and the public clonotype TRBV6.1-TRBJ2-7 CASSLGQAYEQYF

Downloaded from http://www.jimmunol.org/ by guest on February 24, 2022

found in three of three subjects was in agreement with previous studies (6, 41). The presence of public clonotypes and the global restriction of repertoire cannot be only attributed to the successive and repetitive stimulations of immune cells upon chronic infection, as the above public clonotype appeared early during acute infection (41, 42). Different studies have also suggested that the structural constraints/mechanisms of the TCR–pMHC interaction (12, 13, 43, 44) and the endogenous selection of T cells (45) might play an important role in the regulation of the level of TCR diversity. With regard to the biological relevance, it has recently been reported that the number of public clonotypes within CD8 T cells responding to an epitope known as protective in SIV infection (46) was correlated with a better outcome of virus infection (47). Of note, we have also identified two novel public clonotypes in response to $EBV_{RAKFKQLL}$ and $EBV_{GLCTLVAML}$.

The TRB repertoire emerging upon HIV-1 infection was also characterized by a large diversity similar to or even greater in magnitude than that observed in response to CMV- and EBV-derived epitopes.

It has recently been reported that the TCR diversity remains stable over time in controlled virus infections such as CMV (48). However, the large TCR diversity may be relevant for several reasons and particularly in chronic virus infections after repeated and high levels of Ag exposure. A larger TCR repertoire may warrant limited risk of CD8 T cell clones deletion upon chronic antigenic stimulation by providing an unlimited number of T cell clones expressing TCRs specific to the same antigenic epitope. In the current study, the longitudinal changes in the TRB repertoire in HIV-1–infected subjects support the above considerations. We have observed the occurrence of a massive renewal (i.e., $\leq$80% of the TRB repertoire) after treatment interruption and re-exposure to high Ag levels. A higher rate of clonotypes turnover has been shown to occur in certain HIV-specific CD8 T cell populations (49). As already suggested (49), one can speculate that the large renewal of TRB repertoire resulting from the disappearance of T cell clonotypes and the emergence of new clonotypes upon Ag exposure is due to the adaptation of the T cell repertoire to viral variation and/or to clonal senescence. Most likely, the newly appeared CD8 T cell clonotypes detected after Ag re-exposure might be recruited also from the naive pool. The massive renewal of the TRB repertoire was associated either with the persistence or with major increase in the magnitude of the CD8 T cell-specific responses.

A large TCR diversity comprising clonotypes with different avidity for the cognate epitope may also represent a mechanism for the selection of TCR clonotypes with increased avidity after repetitive Ag exposure to cope more efficiently with the re-encounter virus. Higher TCR avidity has been proposed to be critical for the control of viral infections (50–52) or subsequent infections with related pathogens (40). Of note, we have also shown that the large TRB repertoire renewal observed after treatment interruption and Ag re-exposure may be associated with the increase of functional avidity of T cell recognition. Whereas somatic hypermutation of Igs is the mechanism leading to the generation and selection of Ig-bearing B cells with greater avidity for the cognate Ag, similar mechanisms do not operate in T cells. On the basis of the results shown in this article, one may speculate that the greater TRB repertoire diversity and the massive renewal observed after Ag re-exposure provide the mechanistic basis for the generation of a large number of clonotypes. The screening of a large number of clonotypes may be necessary for the selection eventually of clonotypes with greater avidity for the cognate Ag.

It has been proposed that a highly diverse T cell repertoire able to target multiple epitopes will minimize the selection pressure driving escape mutations (53), will be more efficient to recognize a diverse range of epitope variants (54), and will be theoretically more prone to control virus variants and to confer protective antiviral immunity (53). A highly diverse TCR repertoire provides also the scientific rationale for the existence of several positive and negative regulatory mechanisms of the T cell response (55).

The estimates of the TCR diversity reported in the current study are based on the analysis of the TRB repertoire in memory CD8 T cell populations. It is highly likely that the TCR α-chain repertoire and the absence of Ag-driven selection in naive T cell populations are both factors that may sensibly increase the TCR diversity. It is therefore conceivable that the TCR diversity may even be substantially greater.

In conclusion, the current study provides new ground for better understanding TCR diversity. The greater TCR diversity may represent a mechanism for the large renewal of the TCR repertoire occurring during chronic virus infection and continuous Ag stimulation and for the selection of virus-specific CD8 T cell responses with greater avidity for the cognate Ag.

Acknowledgments

We thank Drs. Valérie Dutoit and Dietmar Zehn for helpful discussion, G. Gonzalez for excellent assistance with flow cytometry cell sorting, Ester B.M. Remmerswaal for technical help, and Mohamed Faouzi for statistical analysis. We are very grateful to Dr. Pierre-Alexandre Bart and the staff and patients of the clinics that provided blood samples.

Disclosures

The authors have no financial conflicts of interest.

References

1. Garcia, K. C., L. Teyton, and I. A. Wilson. 1999. Structural basis of T cell recognition. *Annu. Rev. Immunol.* 17: 369–397.
2. Correia-Neves, M., C. Waltzinger, D. Mathis, and C. Benoist. 2001. The shaping of the T cell repertoire. *Immunity* 14: 21–32.
3. Sim, B. C., L. Zerva, M. I. Greene, and N. R. Gascoigne. 1996. Control of MHC restriction by TCR Valpha CDR1 and CDR2. *Science* 273: 963–966.
4. Lichterfeld, M., X. G. Yu, S. Le Gall, and M. Altfeld. 2005. Immunodominance of HIV-1-specific CD8(+) T-cell responses in acute HIV-1 infection: at the crossroads of viral and host genetics. *Trends Immunol.* 26: 166–171.
5. Yewdell, J. W., and M. Del Val. 2004. Immunodominance in TCD8+ responses to viruses: cell biology, cellular immunology, and mathematical models. *Immunity* 21: 149–153.
6. Argaet, V. P., C. W. Schmidt, S. R. Burrows, S. L. Silins, M. G. Kurilla, D. L. Doolan, A. Suhrbier, D. J. Moss, E. Kieff, T. B. Sculley, and I. S. Misko. 1994. Dominant selection of an invariant T cell antigen receptor in response to persistent infection by Epstein-Barr virus. *J. Exp. Med.* 180: 2335–2340.
7. Morrison, J., J. Elvin, F. Latron, F. Gotch, R. Moots, J. L. Strominger, and A. McMichael. 1992. Identification of the nonamer peptide from influenza A matrix protein and the role of pockets of HLA-A2 in its recognition by cytotoxic T lymphocytes. *Eur. J. Immunol.* 22: 903–907.
8. Steven, N. M., N. E. Annels, A. Kumar, A. M. Leese, M. G. Kurilla, and A. B. Rickinson. 1997. Immediate early and early lytic cycle proteins are frequent targets of the Epstein-Barr virus-induced cytotoxic T cell response. *J. Exp. Med.* 185: 1605–1617.
9. Wills, M. R., A. J. Carmichael, K. Mynard, X. Jin, M. P. Weekes, B. Plachter, and J. G. Sissons. 1996. The human cytotoxic T-lymphocyte (CTL) response to cytomegalovirus is dominated by structural protein pp65: frequency, specificity, and T-cell receptor usage of pp65-specific CTL. *J. Virol.* 70: 7569–7579.
10. Turner, S. J., P. C. Doherty, J. McCluskey, and J. Rossjohn. 2006. Structural determinants of T-cell receptor bias in immunity. *Nat. Rev. Immunol.* 6: 883–894.
11. Moss, P. A., R. J. Moots, W. M. Rosenberg, S. J. Rowland-Jones, H. C. Bodmer, A. J. McMichael, and J. I. Bell. 1991. Extensive conservation of alpha and beta chains of the human T-cell antigen receptor recognizing HLA-A2 and influenza A matrix peptide. *Proc. Natl. Acad. Sci. USA* 88: 8987–8990.
12. Kjer-Nielsen, L., C. S. Clements, A. W. Purcell, A. G. Brooks, J. C. Whisstock, S. R. Burrows, J. McCluskey, and J. Rossjohn. 2003. A structural basis for the selection of dominant alphabeta T cell receptors in antiviral immunity. *Immunity* 18: 53–64.
13. Stewart-Jones, G. B., A. J. McMichael, J. I. Bell, D. I. Stuart, and E. Y. Jones. 2003. A structural basis for immunodominant human T cell receptor recognition. *Nat. Immunol.* 4: 657–663.
14. Busch, D. H., I. Pilip, and E. G. Pamer. 1998. Evolution of a complex T cell receptor repertoire during primary and recall bacterial infection. *J. Exp. Med.* 188: 61–70.

Downloaded from http://www.jimmunol.org/ by guest on February 24, 2022

15. Trautmann, L., M. Rimbert, K. Echasserieau, X. Saulquin, B. Neveu, J. Dechanet, V. Cerundolo, and M. Bonneville. 2005. Selection of T cell clones expressing high-affinity public TCRs within Human cytomegalovirus-specific CD8 T cell responses. *J. Immunol.* 175: 6123–6132.
16. Callan, M. F., N. Annels, N. Steven, L. Tan, J. Wilson, A. J. McMichael, and A. B. Rickinson. 1998. T cell selection during the evolution of CD8+ T cell memory in vivo. *Eur. J. Immunol.* 28: 4382–4390.
17. Lin, M. Y., and R. M. Welsh. 1998. Stability and diversity of T cell receptor repertoire usage during lymphocytic choriomeningitis virus infection of mice. *J. Exp. Med.* 188: 1993–2005.
18. Sourdive, D. J., K. Murali-Krishna, J. D. Altman, A. J. Zajac, J. K. Whitmire, C. Pannetier, P. Kourilsky, B. Evavold, A. Sette, and R. Ahmed. 1998. Conserved T cell receptor repertoire in primary and memory CD8 T cell responses to an acute viral infection. *J. Exp. Med.* 188: 71–82.
19. Price, D. A., J. M. Brenchley, L. E. Ruff, M. R. Betts, B. J. Hill, M. Roederer, R. A. Koup, S. A. Migueles, E. Gostick, L. Wooldridge, et al. 2005. Avidity for antigen shapes clonal dominance in CD8+ T cell populations specific for persistent DNA viruses. *J. Exp. Med.* 202: 1349–1361.
20. Venturi, V., H. Y. Chin, T. E. Asher, K. Ladell, P. Scheinberg, E. Bornstein, D. van Bockel, A. D. Kelleher, D. C. Douek, D. A. Price, and M. P. Davenport. 2008. TCR beta-chain sharing in human CD8+ T cell responses to cytomegalovirus and EBV. *J. Immunol.* 181: 7853–7862.
21. Weekes, M. P., M. R. Wills, K. Mynard, A. J. Carmichael, and J. G. Sissons. 1999. The memory cytotoxic T-lymphocyte (CTL) response to human cytomegalovirus infection contains individual peptide-specific CTL clones that have undergone extensive expansion in vivo. *J. Virol.* 73: 2099–2108.
22. Lim, A., L. Trautmann, M. A. Peyrat, C. Couedel, F. Davodeau, F. Romagné, P. Kourilsky, and M. Bonneville. 2000. Frequent contribution of T cell clonotypes with public TCR features to the chronic response against a dominant EBV-derived epitope: application to direct detection of their molecular imprint on the human peripheral T cell repertoire. *J. Immunol.* 165: 2001–2011.
23. Khan, N., N. Shariff, M. Cobbold, R. Bruton, J. A. Ainsworth, A. J. Sinclair, L. Nayak, and P. A. Moss. 2002. Cytomegalovirus seropositivity drives the CD8 T cell repertoire toward greater clonality in healthy elderly individuals. *J. Immunol.* 169: 1984–1992.
24. Lichterfeld, M., X. G. Yu, S. K. Mui, K. L. Williams, A. Trocha, M. A. Brockman, R. L. Allgaier, M. T. Waring, T. Koibuchi, M. N. Johnston, et al. 2007. Selective depletion of high-avidity human immunodeficiency virus type 1 (HIV-1)-specific CD8+ T cells after early HIV-1 infection. *J. Virol.* 81: 4199–4214.
25. Rizzardi, G. P., A. Harari, B. Capiluppi, G. Tambussi, K. Ellefsen, D. Ciuffreda, P. Champagne, P. A. Bart, J. P. Chave, A. Lazzarin, and G. Pantaleo. 2002. Treatment of primary HIV-1 infection with cyclosporin A coupled with highly active antiretroviral therapy. *J. Clin. Invest.* 109: 681–688.
26. Frahm, N., B. Baker, and C. Brander. 2008. Identification and optimal definition of HIV-derived cytotoxic T lymphocyte (CTL) epitopes for the study of CTL escape, functional avidity and viral evolution. In HIV Molecular Immunology 2008. B. T. Korber, C. Brander, B. F. Haynes, R. Koup, J. P. Moore, B. D. Walker, and D. I. Watkins, eds. Los Alamos National Laboratory, Theoretical Biology and Biophysics, Los Alamos, NM, p. 3–24.
27. Bart, P. A., R. Goodall, T. Barber, A. Harari, A. Guimaraes-Walker, M. Khonkarly, N. C. Sheppard, Y. Bangala, M. J. Frachette, R. Wagner, et al; EuroVacc Consortium. 2008. EV01: a phase I trial in healthy HIV negative volunteers to evaluate a clade C HIV vaccine, NYVAC-C undertaken by the EuroVacc Consortium. *Vaccine* 26: 3153–3161.
28. Maślanka, K., T. Piatek, J. Gorski, M. Yassai, and J. Gorski. 1995. Molecular analysis of T cell repertoires. Spectratypes generated by multiplex polymerase chain reaction and evaluated by radioactivity or fluorescence. *Hum. Immunol.* 44: 28–34.
29. Wei, S., P. Charmley, M. A. Robinson, and P. Concannon. 1994. The extent of the human germline T-cell receptor V beta gene segment repertoire. *Immunogenetics* 40: 27–36.
30. Liu, J., and D. K. Dey. 2007. Hierarchical overdispersed poisson model with macrolevel autocorrelation. *Stat. Methodol.* 4: 354–370.
31. Ismail, N., and A. A. Jemain. 2007. *Handling Overdispersion with Negative Binomial and Generalized Poisson Regression Model.* Casualty Actuarial Society Forum, Arlington, VA, p. 103–158.
32. Christensen, O. F., and R. Waagepetersen. 2002. Bayesian prediction of spatial count data using generalized linear mixed models. *Biometrics* 58: 280–286.
33. Wood, G. R. 2005. Confidence and prediction intervals for generalised linear accident models. *Accid. Anal. Prev.* 37: 267–273.
34. Royston, P., G. Ambler, and W. Sauerbrei. 1999. The use of fractional polynomials to model continuous risk variables in epidemiology. *Int. J. Epidemiol.* 28: 964–974.
35. Kedzierska, K., E. B. Day, J. Pi, S. B. Heard, P. C. Doherty, S. J. Turner, and S. Perlman. 2006. Quantification of repertoire diversity of influenza-specific epitopes with predominant public or private TCR usage. *J. Immunol.* 177: 6705–6712.
36. Pewe, L. L., J. M. Netland, S. B. Heard, and S. Perlman. 2004. Very diverse CD8 T cell clonotypic responses after virus infections. *J. Immunol.* 172: 3151–3156.
37. Rudd, B. D., V. Venturi, M. J. Smithey, S. S. Way, M. P. Davenport, and J. Nikolich-Zugich. 2010. Diversity of the CD8+ T cell repertoire elicited against an immunodominant epitope does not depend on the context of infection. *J. Immunol.* 184: 2958–2965.
38. Turner, S. J., G. Diaz, R. Cross, and P. C. Doherty. 2003. Analysis of clonotype distribution and persistence for an influenza virus-specific CD8+ T cell response. *Immunity* 18: 549–559.
39. Vigan, I., E. Jouvin-Marche, V. Leroy, M. Pernollet, S. Tongiani-Dashan, E. Borel, E. Delachanal, M. Colomb, J. P. Zarski, and P. N. Marche. 2003. T lymphocytes infiltrating the liver during chronic hepatitis C infection express a broad range of T-cell receptor beta chain diversity. *J. Hepatol.* 38: 651–659.
40. Zehn, D., S. Y. Lee, and M. J. Bevan. 2009. Complete but curtailed T-cell response to very low-affinity antigen. *Nature* 458: 211–214.
41. Callan, M. F., N. Steven, P. Krausa, J. D. Wilson, P. A. Moss, G. M. Gillespie, J. I. Bell, A. B. Rickinson, and A. J. McMichael. 1996. Large clonal expansions of CD8+ T cells in acute infectious mononucleosis. *Nat. Med.* 2: 906–911.
42. Aebischer, T., S. Oehen, and H. Hengartner. 1990. Preferential usage of V alpha 4 and V beta 10 T cell receptor genes by lymphocytic choriomeningitis virus glycoprotein-specific H-2Db-restricted cytotoxic T cells. *Eur. J. Immunol.* 20: 523–531.
43. Tynan, F. E., D. Elhassen, A. W. Purcell, J. M. Burrows, N. A. Borg, J. J. Miles, N. A. Williamson, K. J. Green, J. Tellam, L. Kjer-Nielsen, et al. 2005. The immunogenicity of a viral cytotoxic T cell epitope is controlled by its MHC-bound conformation. *J. Exp. Med.* 202: 1249–1260.
44. Venturi, V., D. A. Price, D. C. Douek, and M. P. Davenport. 2008. The molecular basis for public T-cell responses? *Nat. Rev. Immunol.* 8: 231–238.
45. Burrows, S. R., S. L. Silins, D. J. Moss, R. Khanna, I. S. Misko, and V. P. Argaet. 1995. T cell receptor repertoire for a viral epitope in humans is diversified by tolerance to a background major histocompatibility complex antigen. *J. Exp. Med.* 182: 1703–1715.
46. Casimiro, D. R., F. Wang, W. A. Schleif, X. Liang, Z. Q. Zhang, T. W. Tobery, M. E. Davies, A. B. McDermott, D. H. O'Connor, A. Fridman, et al. 2005. Attenuation of simian immunodeficiency virus SIVmac239 infection by prophylactic immunization with dna and recombinant adenoviral vaccine vectors expressing Gag. *J. Virol.* 79: 15547–15555.
47. Price, D. A., T. E. Asher, N. A. Wilson, M. C. Nason, J. M. Brenchley, I. S. Metzler, V. Venturi, E. Gostick, P. K. Chattopadhyay, M. Roederer, et al. 2009. Public clonotype usage identifies protective Gag-specific CD8+ T cell responses in SIV infection. *J. Exp. Med.* 206: 923–936.
48. Iancu, E. M., P. Corthesy, P. Baumgaertner, E. Devevre, V. Voelter, P. Romero, D. E. Speiser, and N. Rufer. 2009. Clonotype selection and composition of human CD8 T cells specific for persistent herpes viruses varies with differentiation but is stable over time. *J. Immunol.* 183: 319–331.
49. Almeida, J. R., D. A. Price, L. Papagno, Z. A. Arkoub, D. Sauce, E. Bornstein, T. E. Asher, A. Samri, A. Schnuriger, I. Theodorou, et al. 2007. Superior control of HIV-1 replication by CD8+ T cells is reflected by their avidity, polyfunctionality, and clonal turnover. *J. Exp. Med.* 204: 2473–2485.
50. Alexander-Miller, M. A., G. R. Leggatt, and J. A. Berzofsky. 1996. Selective expansion of high- or low-avidity cytotoxic T lymphocytes and efficacy for adoptive immunotherapy. *Proc. Natl. Acad. Sci. USA* 93: 4102–4107.
51. Messaoudi, I., J. A. Guevara Patiño, R. Dyall, J. LeMaoult, and J. Nikolich-Zugich. 2002. Direct link between mhc polymorphism, T cell avidity, and diversity in immune defense. *Science* 298: 1797–1800.
52. Speiser, D. E., D. Kyburz, U. Stübi, H. Hengartner, and R. M. Zinkernagel. 1992. Discrepancy between in vitro measurable and in vivo virus neutralizing cytotoxic T cell reactivities. Low T cell receptor specificity and avidity sufficient for in vitro proliferation or cytotoxicity to peptide-coated target cells but not for in vivo protection. *J. Immunol.* 149: 972–980.
53. Price, D. A., S. M. West, M. R. Betts, L. E. Ruff, J. M. Brenchley, D. R. Ambrozak, Y. Edghill-Smith, M. J. Kuroda, D. Bogdan, K. Kunstman, et al. 2004. T cell receptor recognition motifs govern immune escape patterns in acute SIV infection. *Immunity* 21: 793–803.
54. Douek, D. C., M. R. Betts, J. M. Brenchley, B. J. Hill, D. R. Ambrozak, K. L. Ngai, N. J. Karandikar, J. P. Casazza, and R. A. Koup. 2002. A novel approach to the analysis of specificity, clonality, and frequency of HIV-specific T cell responses reveals a potential mechanism for control of viral escape. *J. Immunol.* 168: 3099–3104.
55. Blackburn, S. D., H. Shin, W. N. Haining, T. Zou, C. J. Workman, A. Polley, M. R. Betts, G. J. Freeman, D. A. Vignali, and E. J. Wherry. 2009. Coregulation of CD8+ T cell exhaustion by multiple inhibitory receptors during chronic viral infection. *Nat. Immunol.* 10: 29–37.

Downloaded from http://www.jimmunol.org/ by guest on February 24, 2022